BIFURCATIONS IN ANNULUS-LIKE PARAMETER SPACE OF DELAYED-PWM SWITCHED CONVERTER

F. Angulo, G. Olivar, J.A. Taborda
Department of Electrical and Electronics Engineering, and Computer Science
Universidad Nacional de Colombia - Sede Manizales
Colombia
fangulog@unal.edu.co, golivart@unal.edu.co, yatabordag@unal.edu.co

Abstract
In this paper, we propose a study about bifurcations and chaos in Digital Delayed Pulse-Width Modulator (PWM) switched converters. The Digital-PWM is based on Zero Average Dynamic (ZAD) strategy and a one-period delay in the control law is included . The control parameter of the ZAD strategy (k_s) is varied in the whole range $(-\infty, \infty)$. In the limits, the dynamical behavior is the same, yielding an annulus-like parameter space. High richness of dynamics is obtained. Periodic orbits, periodic windows, period-adding cascades, border-collision bifurcations, chaotic bands and chaos are possible depending on the k_s value. The switched converter is modelled as a piecewise linear system where the analytical equation of the Poincaré map is available.

Key words
Bifurcation theory, border-collision, chaos, period-adding, switched systems, delayed systems.

1 Introduction

Switched converters can be modelled as piecewise smooth systems (Olivar and Fossas, 1996), (Di Bernardo *et al.*, 1998*a*). The dynamical behavior of these systems has been extensively studied, in practical (Deane and Hamill, 1990), (Yuan and Banerjee, 1998) and theoretical researches (Olivar, 1997), (Di Bernardo and Tse, 2002).

Many phenomena in power converters cannot be explained using the smooth bifurcations approach (for example, (El Aroudi *et al.*, 2005) or (Zhusubaliyev *et al.*, 2003)), therefore, it is necessary to incorporate the concepts of nonsmooth theory and the discontinuity induced bifurcations (DIBs) approach (Di Bernardo *et al.*, 1998*b*), (Di Bernardo *et al.*, 2001), (Banerjee and Grebogi, 2002), (Di Bernardo *et al.*, 2006), (Piiroinen *et al.*, 2004).

Digital-PWM controllers are a novel alternative to control power converters. In this paper, we use the Digital-PWM based in *Zero Average Dynamic* or *ZAD strategy* that was proposed very recently in (Fossas *et al.*, 2003), (Angulo, 2004).

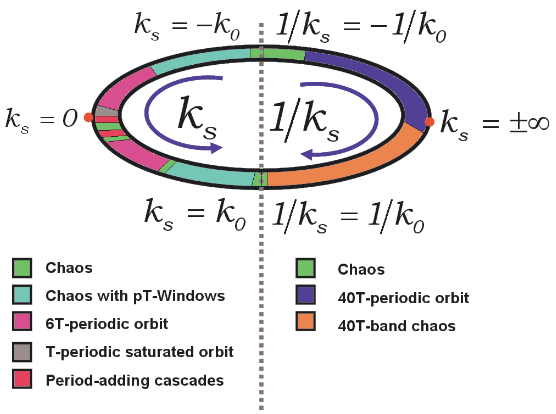

Figure 1. Annulus-like parameter space. Qualitative distribution of the nonlinear phenomena. Two bifurcation parameters: k_s and $1/k_s$. Two ranges of analysis: $-k_0 < k_s < k_0$ and $-k_0^{-1} < k_s^{-1} < k_0^{-1}$ with $k_0 = 100$.

Bifurcational analysis of PWM switched converters based on ZAD strategy was done in (Angulo, 2004), (Angulo *et al.*, 2005) and (Angulo *et al.*, 2008) for real-time operation, i.e., without delay time. In (Taborda, 2004), this converter was studied with one-period delay. Different routes to chaos can be observed depending on the delay time in the control law, when the ZAD control parameter (k_s) is varied. For example, without delay time, the transition to chaos is influenced by period-doubling and border collision phenomena and denoted as border collision period-doubling bifurcation scenario (Angulo *et al.*, 2005).

With one-period delay, different transitions to chaos can be presented depending on the range of the k_s parameter. Since the ZAD controller is implemented in digital platforms, the k_s value can be selected in an extensive range. Ideally, this range can be $(-\infty, \infty)$. In the limits (i.e., $-\infty$ or ∞), the dynamical behavior is the same, yielding an annulus-like parameter space. The qualitative distribution of the nonlinear phenomena in the annulus-like parameter space is presented in Fig.1. High richness of dynamics is obtained. Periodic orbits, periodic windows, period-adding cascades, border-collision bifurcations, chaotic bands and chaos are possible depending on the evaluated range. To analyze the whole k_s range, two bifurcation parameters are used (k_s and $1/k_s$) and two ranges of analysis are defined: $-k_0 < k_s < k_0$ and $-k_0^{-1} < k_s^{-1} < k_0^{-1}$ where k_0 is a real constant.

In this paper, we present a general description of the bifurcational behavior in the whole k_s range. The main characteristic is the presence of border-collision scenarios. Nowadays, these scenarios are widely studied. For example, in (Avrutin and Schanz, 2005) and (Avrutin *et al.*, 2007) the influence of the border-collision bifurcations in period-doubling scenario without flip bifurcations and the border-collision in the three-codimension approach are studied.

2 Delayed-PWM Switched Converter Modelling

The buck converter (shown in Fig.2) can be described by the state-space representation of equation (1).

$$\begin{bmatrix} \dot{v} \\ \dot{i} \end{bmatrix} = \begin{bmatrix} -\frac{1}{RC} & \frac{1}{C} \\ -\frac{1}{L} & 0 \end{bmatrix} \begin{bmatrix} v \\ i \end{bmatrix} + \begin{bmatrix} 0 \\ \frac{E}{L} \end{bmatrix} u \qquad (1)$$

The capacitor voltage v and the inductor current i are the state variables. The control signal u takes discrete values in the set $\{-1, 1\}$, in each cycle. Depending on u, the RLC circuit is fed with $+E$ or $-E$ voltage. The parameters values used are: $R = 20\Omega$, $C = 40\mu F$, $L = 2mH$, $E = 40V$ and a sampling period of $T_c = 50\mu s$. With the following change of variables

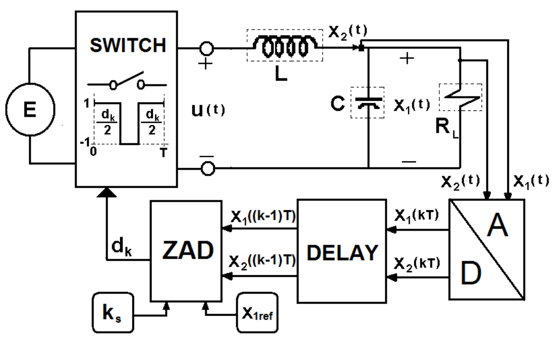

Figure 2. Digital Delayed PWM Switched converter: input (E), PWM-controlled switch, LC filter, R load, analog/digital converter, delay block and ZAD controller where k_s is the control parameter and x_{1ref} is the desired value in the output.

in Eq.(1): $x_1 = v/E$, $x_2 = (1/E)\sqrt{(L/C)}\,i$, and $t = \tau \big/ \sqrt{LC}$ we achieve dimensionless variables and parameters (Fossas and Zinober, 2001). Therefore, the Buck converter can be modelled using the piecewise-linear switching system given in Eq.(2).

$$\begin{bmatrix} \dot{x}_1 \\ \dot{x}_2 \end{bmatrix} = \begin{bmatrix} -\gamma & 1 \\ -1 & 0 \end{bmatrix} \begin{bmatrix} x_1 \\ x_2 \end{bmatrix} + \begin{bmatrix} 0 \\ 1 \end{bmatrix} u \qquad (2)$$

where, γ is a dimensionless parameter, related to the physical parameters of the Buck converter:

$$\gamma = \frac{1}{R_L}\sqrt{\frac{L}{C}}$$

The control signal $u(t)$ is defined in (3) where centered pulses are present in each sampling period (T) related to the duty cycle (d_k), with $T = T_c \big/ \sqrt{LC} = 0.1767$ and $d_k \in [\,0\,,\,T\,]$.

$$u = \begin{cases} 1 & \text{if} \quad kT \leqslant t \leqslant kT + d_k/2 \\ -1 & \text{if} \quad kT + d_k/2 < t < kT + (T - d_k/2) \\ 1 & \text{if} \quad kT + (T - d_k/2) \leqslant t \leqslant (k+1)\,T \end{cases} \qquad (3)$$

In Eq.(4), the centered-PWM signal (given in (3)) is applied to the system: $\dot{\mathbf{x}} = \mathbf{Ax} + \mathbf{Bu(t)}$. For simplicity, in Eq.(4) only the first iteration is considered.

$$\dot{\mathbf{x}} = \begin{cases} \mathbf{Ax} + \mathbf{B} & \text{if} \quad 0 \le t \le \frac{d_k}{2} \\ \mathbf{Ax} - \mathbf{B} & \text{if} \quad \frac{d_k}{2} < t < (T - \frac{d_k}{2}) \\ \mathbf{Ax} + \mathbf{B} & \text{if} \quad (T - \frac{d_k}{2}) \le t \le T \end{cases} \qquad (4)$$

This system will be controlled with PWM in order to achieve, in every T-cycle, a zero average in the error dynamics $s(\mathbf{x})$, which is defined as

$$s(\mathbf{x}) = x_1 - x_{1ref} + k_s(\dot{x}_1 - \dot{x}_{1ref}).$$

x_1 is the variable to be controlled, x_{1ref} is the reference signal and k_s is the time constant associated to the first order dynamics given by the surface. This guarantees also that the output x_1 follows the reference x_{1ref}. Note that in our case, $\dot{x}_{1ref} = 0$, since we will assume that x_{1ref} is constant.

Computing the exact switching time d_k (the duty cycle) implies, in each cycle iteration, solving a transcendental equation, and that is a serious inconvenient in practice. In order to simplify the duty cycle computation, $s(\mathbf{x})$ was approximated to a piecewise linear function (Angulo, 2004). This function is presented in Eq.(5).

$$s_{pwl}(t) = \begin{cases} \dot{s}_1\,(kT)\,t + s_1(kT) & if \quad 0 \le t \le \frac{d_k}{2} \\ \dot{s}_2\,(kT)\,t + s_2(kT) & if \quad \frac{d_k}{2} < t < (T - \frac{d_k}{2}) \\ \dot{s}_1\,(kT)\,t + s_3(kT) & if \quad (T - \frac{d_k}{2}) \le t \le T \end{cases} \qquad (5)$$

where $\dot{s}_1$ and $\dot{s}_2$ are the slopes of the lateral and central pieces of s_{pwl}, respectively. Also, $s_1(kT) = s(kT)$

is the value of the function $s(t)$ at each sampling instant; $s_2(kT) = s(kT) + (d_k/2)\left(\dot{s}_1(kT) - \dot{s}_2(kT)\right)$ and $s_3(kT) = s(kT) - (T - d_k)\left(\dot{s}_1(kT) - \dot{s}_2(kT)\right)$. Therefore, the zero average criterion is applied to Eq.(6) where it is possible to obtain an algebraic expression for computing d_k. This equation is given in (7).

$$\int_{kT}^{(k+1)T} s_{pwl}(t)dt = 0 \tag{6}$$

$$d_k = \frac{2s\left(kT\right) + T\dot{s}_2\left(kT\right)}{\dot{s}_2\left(kT\right) - \dot{s}_1\left(kT\right)} \tag{7}$$

Equation (7) can be written as a function of the state variables x_1 and x_2 in the sampling instant kT: $d_k = c_1x_1\left(kT\right) + c_2x_2\left(kT\right) + c_3$ where

$$c_1 = \left[\left(2 - 2\gamma k_s + \gamma^2 k_s T - \gamma T - k_s T\right)/(-2k_s)\right],$$

$$c_2 = \left[(2k_s + T - \gamma k_s T)/(-2k_s)\right],$$

$$c_3 = \left[(x_{1ref}/k_s) + (T/2)\right].$$

If the PWM controller is delayed, the duty cycle is computed with the one-period delay state variables x_1 and x_2, which are given in (8).

$$d_k = c_1x_1\left((k-1)T\right) + c_2x_2\left((k-1)T\right) + c_3 \tag{8}$$

The dimensionless parameters associated to the system are γ, k_s, x_{1ref} and T. We fix $\gamma = 0.35$, $T = 0.1767$, $x_{1ref} = 0.8$ and we will vary parameter k_s. These values correspond to a experimental prototype reported in (Angulo *et al.*, 2006).

3 Analysis based on Poincaré Maps

The Delayed-PWM switched converter presented in the previous section will be analyzed using Poincaré Maps, which are defined analytically.

First, the continuous solution of the converter is presented. Later, the T-periodic Poincaré map is computed and the discontinuity boundaries are defined. Using the Poincaré map, the bifurcation diagram is computed for two analysis ranges: $-k_0 < k_s < k_0$ and $-k_0^{-1} < k_s^{-1} < k_0^{-1}$ where k_0 is a real constant. For very high k_s values an auxiliar bifurcation parameter ($1/k_s$) is used. If we increase the value $1/k_s$ from 0 to $1/k_0$ it is possible to study the bifurcational behavior in the range $k_s \in (k_0, \infty)$.

One point in the state variable bifurcation diagram means a T-periodic orbit. In general, p points in the state variable bifurcation diagram mean a pT-periodic orbit. Many points for the same value of k_s mean that quasiperiodic orbits, chaotic bands or chaos are present. In the duty cycle bifurcation diagram, q points with $q < p$ can mean a pT-periodic orbit due to saturated cycles. The border-collision scenario is more clearly visualized in the duty cycle bifurcation diagram.

3.1 Solution of the system

The solution of the switched converter with Centered-PWM can be computed explicitly, through direct integration. The states $\mathbf{x}(t)$ are defined, in each iteration, as a function of the initial condition $\mathbf{x}(kT)$ and the duty cycle (d_k, which is a function of $\mathbf{x}((k-1)T)$). The solution is presented in Eq.(9) where $\mathbf{A} = \left[-\gamma\ 1\ ;\ -1\ 0\right]$; $\mathbf{B} = [0;\ 1]$; $\mathbf{v}_1 = \mathbf{x}\left(kT\right) + \mathbf{A}^{-1}\mathbf{B}$; $\mathbf{v}_2 = \mathbf{v}_1 + 2e^{-\mathbf{A}(d_k/2)}\mathbf{A}^{-1}\mathbf{B}$ and $\mathbf{v}_3 = \mathbf{v}_2 + 2e^{-\mathbf{A}(T-d_k/2)}\mathbf{A}^{-1}\mathbf{B}$.

$$\mathbf{x}(t) = \begin{cases} e^{\mathbf{A}t}\mathbf{v}_1 - \mathbf{A}^{-1}\mathbf{B} \text{ if } & 0 \le t \le \frac{d_k}{2} \\ e^{\mathbf{A}t}\mathbf{v}_2 + \mathbf{A}^{-1}\mathbf{B} \text{ if } & \frac{d_k}{2} < t < (T - \frac{d_k}{2}) \\ e^{\mathbf{A}t}\mathbf{v}_3 - \mathbf{A}^{-1}\mathbf{B} \text{ if } & (T - \frac{d_k}{2}) \le t \le T \end{cases} \tag{9}$$

The flow generated by the solutions of the systems can describe different trajectories types. Three options of duty cycles are possible: non-saturated cycles $0 < d_k < T$, saturated cycles in $d_k = 0$ and saturated cycles in $d_k = T$. Next, we will study its Poincaré or stroboscopic map.

3.2 Poincaré Map

Let Π be the Poincaré map of the T-periodic orbit of the system (2): Π : $\mathbf{x}_0 \mapsto \Pi\left(\mathbf{x}_0\right)$. The discrete solution equivalent to Poincaré map Π, can be obtained through direct integration, and this leads to Eq.(10).

$$\mathbf{x}\left((k+1)\,T\right) = e^{\mathbf{A}T}\mathbf{x}(kT) + \mathbf{f}\left(d_k\left(\mathbf{x}((k-1)T)\right)\right) \tag{10}$$

where $\mathbf{f}_k = \mathbf{f}\left(d_k\left(\mathbf{x}((k-1)T)\right)\right)$ is a vectorial function of d_k, which is given in Eq.(11) with $\mathbf{f}_c = \left[e^{\mathbf{A}T} - \mathbf{I}\right]\mathbf{A}^{-1}\mathbf{B}$ and $\mathbf{f}_d = 2\left(e^{\mathbf{A}(d_k/2)} - e^{\mathbf{A}(T-d_k/2)}\right)\mathbf{A}^{-1}\,\mathbf{B}$.

$$\mathbf{f}_k = \begin{cases} \mathbf{f}_c + \mathbf{f}_d \text{ if } 0 < d_k < T \\ \quad\mathbf{f}_c \quad \text{if} \quad d_k \geqslant T \\ \ -\mathbf{f}_c \quad \text{if} \quad d_k \leqslant 0 \end{cases} \tag{11}$$

Then, the discontinuous piecewise linear vector field can be splitted in three regions of the state space, depending on the condition of the duty cycle (saturated or non-saturated).

4 Results

Next, we show a general description of the bifurcational behavior in the whole k_s range. The main characteristic is the presence of border-collision scenarios. First, we show the bifurcations diagrams based on the Poincaré map for the whole k_s range. Later, we describe three different border-collision scenarios in specific zones of k_s range.

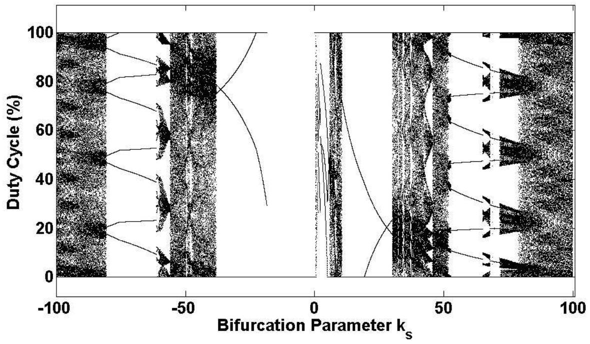

Figure 3. Duty Cycle Bifurcation diagram where k_s is the bifurcation parameter. The analysis range is: $-k_0 < k_s < k_0$ with $k_0 = 100$.

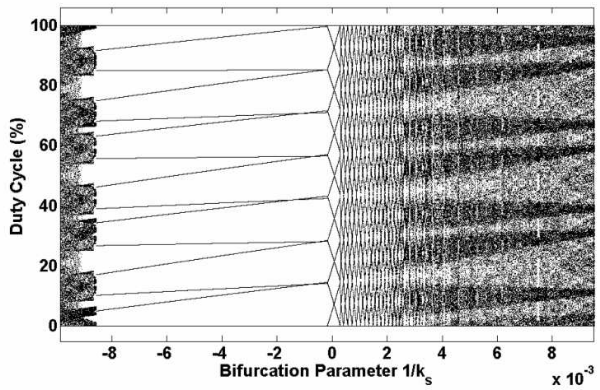

Figure 4. Duty Cycle Bifurcation diagram where $1/k_s$ is the bifurcation parameter. The analysis range is: $-k_0^{-1} < k_s^{-1} < k_0^{-1}$ with $k_0 = 100$.

4.1 General Description of the Bifurcational Behavior

Figures 3 and 4 show the duty cycle bifurcation diagrams for the whole k_s range. In Fig.3, the k_s value is varied in the range $-k_0 < k_s < k_0$ with $k_0 = 100$, while the $1/k_s$ value is varied in the range $-k_0^{-1} < k_s^{-1} < k_0^{-1}$, (see Fig.4).

If we increase the value of k_s, in very small increments of the parameter from $-k_0$ to k_0, then the bifurcation diagram based on the Poincaré map can be obtained using Eq.(10). The more representative (non-rigorous) nonlinear sequence in this range is: Chaos → 23T-periodic orbit → Chaotic bands → Chaos → 6T-periodic orbit → 1T-periodic saturated orbit → Period-adding cascade 1 → Chaos → Period-adding cascade 2 → Chaos → Chaotic Bands → 26T-periodic orbit → 13T-periodic orbit → Chaos → 6T-periodic orbit → Chaos → 23T-periodic orbit → Chaotic bands → Chaos. Other periodic windows are possible but were not considered in this paper.

Next, we show some considerations about the bifurcational behavior in the range $-100 < k_s < 100$ (Fig.3):

- Qualitatively, the range $k_s \in (-18.5; -100)$ has symmetric properties with the range $k_s \in (10.5; 100)$. The sequence: Chaos → 23T-periodic orbit → Chaotic bands → Chaos → 6T-periodic orbit is similar in the two cases.
- The 1T-periodic orbit is stable only for negative k_s values ($k_s \in (0; -18.5)$). This orbit is saturated to $d = 0\%$, therefore it has no practical applications.
- The period-adding cascades are present for positive and close to zero k_s values. Between $k_s = 0$ and $k_s = 0.28$, the following sequence exists: 23T → 22T → 21T → 20T → 19T → ... → 16T. Between $k_s = 0.5$ and $k_s = 30$, the following sequence exists: 12T → 11T → 10T → 9T → 8T → 7T → 6T.
- Period-doubling scenario is possible too. For example in the transition 26T-13T ($k_s \in (5.7; 10.5)$) border-collision bifurcations cause period-doubling phenomena. This fact is similar to the one reported in (Avrutin and Schanz, 2005).

If we increase the value of $1/k_s$, in very small increments of the parameter, from $-1/k_0$ to $1/k_0$, then the bifurcation diagram based on the Poincaré map can be obtained using Eq.(10). The more representative (non-rigorous) nonlinear sequence in this range is: Chaos → Chaotic bands → 40T-periodic orbit → 40T-band chaos → Chaos. The 40T-periodic orbit is stable in a wide range. The border-collision bifurcations cause the birth of the 40T-band chaos and its destruction into full chaos.

Next, we describe three different border-collision scenarios in specific zones of k_s range.

4.2 Scenario 1: Period-adding route to chaos

By reducing the bifurcation parameter from $k_s = 30$, the system shows a 6T-periodic orbit with 2 non-saturated cycles and 4 saturated cycles (one in $d = 0\%$ and three in $d = 100\%$), in the following structure: $d_0 - 0 - d_2 - T - T - T$. At $k_s = 19.2$ a border-collision bifurcation occurs due to the fact that the d_2 cycle reaches the limit $d = 0\%$. Therefore, the new structure is $d_0 - 0 - 0 - T - T - T$ and it persists until $k_s = 10.5$. In the range $k_s \in (5.7; 10.5)$, the system shows chaotic motion with periodic windows. This scenario will be explained in the next section. For

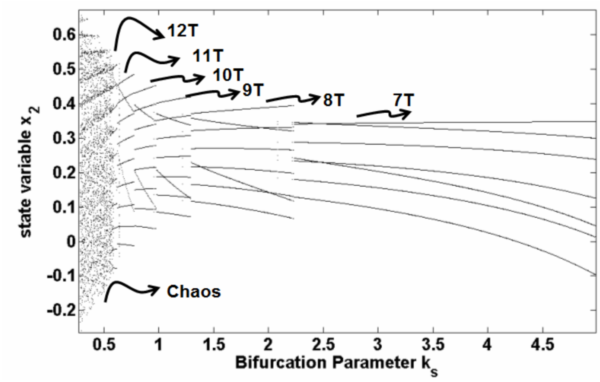

Figure 5. State variable (x_2) Bifurcation diagram where k_s is the bifurcation parameter. The analysis range is: $0.28 < k_s < 5$. Example of Period-adding route to chaos

$k_s = 5.7$, the switched converter shows $7T$-periodic orbits with 2 non-saturated cycles and 5 saturated cycles (one in $d = 0\%$ and four in $d = 100\%$), with the following structure: $d_0 - 0 - d_2 - T - T - T - T$. For $k_s = 4.98$ a border-collision bifurcation occurs and the structure changes to: $d_0 - d_1 - d_2 - T - T - T - T$.

For $k_s = 2.2$ the transition $7T - 8T$ occurs and, after, the system shows a period-adding cascade: $8T - 9T - 10T - 11T - 12T$ in a narrow range ($k_s \in (2.2; 0.5)$). Between $k_s = 0.5$ and $k_s = 0.28$ chaos is present. The duty cycle structure is shown in Eq.(12) where the three non-saturated cycles are kept and $(p-3)$ saturated cycles in $d = 100\%$ appear with $p = 8, 9, ..., 12$.

$$d_0 - d_1 - d_2 - T_1 - T_2 - ... - T_{p-3} \qquad (12)$$

The bifurcation diagram for the state variable (x_2) is presented in Fig.5 for the range $k_s \in (5; 0.28)$.

4.3 Scenario 2: Chaos with periodic windows

Border-collision bifurcations can create period-doubling scenarios, just as it is reported in (Avrutin and Schanz, 2005). In the approximate range $k_s \in (8; 8.33)$, the switched converter has a transition from 13T-periodic orbit $\rightarrow$ 26T-periodic orbit $\rightarrow$ chaos. New border-collision bifurcations in $k_s = (8.009; 8.059; 8.065; 8.254)$ occur in this transition. By reducing the k_s value from 8.33 backwards, the 13T-periodic with the structure $d_0 - 0 - d_2 - T - T - T - T - d_7 - 0 - d_9 - T - T - T$ changes to the structure $d_0 - d_1 - d_2 - T - T - T - T - d_7 - 0 - d_9 - T - T - T$ for $k_s = 8.254$. The border-collision for $k_s = 8.065$ gives rise to a $26T$-periodic orbit and the following bifurcations for $k_s = 8.059$ and $k_s = 8.009$ give rise to chaos.

the duty cycle bifurcation diagram in the range $5.7 < k_s < 10.5$ is presented in Fig.6.

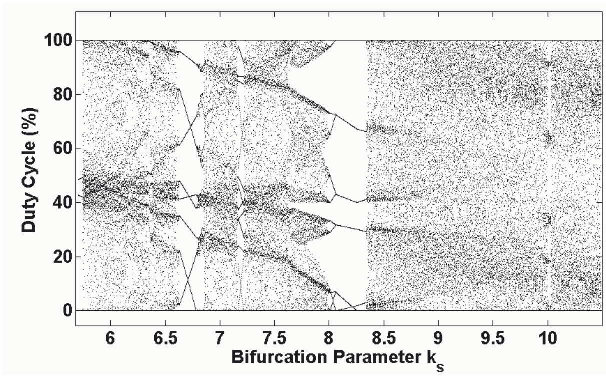

Figure 6. Duty Cycle Bifurcation diagram where k_s is the bifurcation parameter. The analysis range is: $5.7 < k_s < 10.5$. Example of Chaos with periodic windows

4.4 Scenario 3: High-order periodic orbit to chaotic bands to chaos transition

In the range $k_s \in (-117; -\infty)$ and $k_s \in (90; \infty)$ the system has the following transition: 40T-periodic orbit $\rightarrow$ 40T-band chaos $\rightarrow$ chaos. In the limits, (i.e., $-\infty$ or ∞), the system has 40T-periodic orbits giving rise to an annulus-like parameter space. If we increase the

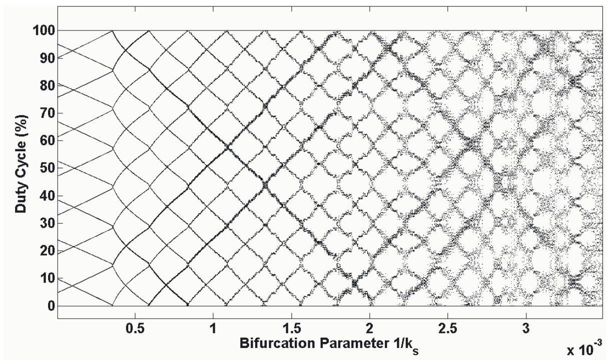

Figure 7. Duty Cycle Bifurcation diagram where $1/k_s$ is the bifurcation parameter. The analysis range is: $0 < k_s^{-1} < 4e^{-3}$. Example of high-order periodic orbit to chaotic bands transition

value of $1/k_s$ from -0.0085, in very small increments of the parameter, then the system has a 40T-periodic orbit with 14 non-saturated cycles , 14 saturated cycles in $d = 0\%$ and 13 saturated cycles in $d = 100\%$. Close to $(1/k_s) = 0$ the structure of the $40T$-periodic orbit changes to 14 non-saturated cycles ,13 saturated cycles in $d = 0\%$ and 13 saturated cycles in $d = 100\%$ due to border-collision bifurcations. After, border-collision bifurcations give rise to 40T-band chaos.

In Fig.7, a border-collision scenario in the birth of the $40T$-band chaos is shown. The interaction of the system with the discontinuity boundaries allow the birth of the chaotic attractor. The characterization of this scenario can be found in (Taborda *et al.*, 2007).

5 Conclusion

A study about bifurcations and chaos is shown in Digital Delayed Pulse-Width Modulator (PWM) switched converters. The control parameter of the ZAD strategy (k_s) has been varied in the whole range $(-\infty, \infty)$. In the limits, the dynamical behavior is the same, creating an annulus-like parameter space. High richness of dynamics has been obtained.

References

Angulo, F. (2004). *Dynamical analisys of PWM-controlled power electronic converters based on the zero average dynamics (ZAD) strategy*. Ph. D. Thesis. Technical University of Catalonia (in Spanish). Barcelone, Spain.

Angulo, F., C. Ocampo, G. Olivar and R. Ramos (2006). Nonlinear and nonsmooth dynamics in a dc–dc buck convreter: two experimental set-ups. *Nonlinear Dynam*.

Angulo, F., E. Fossas and G. Olivar (2005). Transition from periodicity to chaos in a pwm-controlled buck converter with zad strategy. *Interntional Journal of Bifurcations and Chaos (IJBC)*.

Angulo, F., G. Olivar and J.A. Taborda (2008). Continuation of periodic orbits in a zad-strategy controlled buck converter. *Chaos, Solitons and Fractals (article in press)*.

Avrutin, V. and M. Schanz (2005). Period-doubling scenario without flip bifurcations in a one-dimensional map. *International Journal of Bifurcation and Chaos, vol. 15 No. 4*.

Avrutin, V., M. Schanz and S. Banerjee (2007). Codimension-three bifurcations: Explanation of the complex one-, two-, and three-dimensional bifurcation structures in nonsmooth maps. *Physical Review E 75*.

Banerjee, S. and C. Grebogi (2002). Border collision bifurcations at the change of statespace dimension. *Chaos* **12**, 1054–1069.

Deane and Hamill (1990). Analysis, simulation and experimental study of chaos in buck converter. *Proceedings IEEE Power Electronics*.

Di Bernardo, M. and Ch. Tse (2002). Complex behavior in switching power converter. *Proceedings IEEE*.

Di Bernardo, M., C. Budd and A. Champneys (1998*a*). Grazing, skipping and sliding: Analysis of the nonsmooth dynamics of the dc/dc buck converter. *Nonlinearity 11 859–890. Printed in the UK*.

Di Bernardo, M., C. Budd and A. Champneys (1998*b*). Grazing, skipping and sliding: analysis of the nonsmooth dynamics of the dc/dc buck converter.. *Nonlinearity* **11**, 858–890.

Di Bernardo, M., C. Budd and A. Champneys (2001). Grazing and border-collision in piecewise smooth systems: a unified analytical framework.. *Phys. Rev. Lett.* pp. 86:2553–2556.

Di Bernardo, M., C. Budd and et al (2006). *Bifurcation and Chaos in Piecewise-Smooth Dynamical Systems*. Springer-Verlag. London.

El Aroudi, A., M. Debbat, R. Giral, G. Olivar, L. Benadero and E. Toribio (2005). Bifurcations in dc-dc switching converters: review of methods and applications. *International Journal of Bifurcation and Chaos, vol.15, No.5*.

Fossas, E. and A. Zinober (2001). Adaptive tracking control of nonlinear power converters. *Proceedings IFAC workshop on adaptation in control and signal processing*.

Fossas, E., R. Ramos, D. Biel and F. Guinjoan (2003). A fixed-frecuency quasi-siliding control algorithm: Apllication to power inverters design by means of fpga implementation. *IEEE Transactions On Power Electronics*.

Olivar, G. (1997). *Chaos in Buck Converter*. Universidad Politécnica de Cataluña. Spain.

Olivar, G. and E. Fossas (1996). Study of chaos in buck converter. *IEEE Transactions On Circuits and Systems*.

Piiroinen, P.T., L.N. Virgin and A.R. Champneys (2004). Chaos and period-adding; experimental and numerical verification of the grazing bifurcation.. *Journal of Nonlinear Science* pp. 14(4):383–404.

Taborda, J.A. (2004). *Bifurcational analysis in second-order systems with PWM based on the zero average dynamics (ZAD) strategy*. Master Thesis. National University of Colombia (in Spanish). Manizales, Colombia.

Taborda, J.A., F. Angulo and G. Olivar (2007). Fractal-like chaotic bands in border-collision scenario of delayed-pwm switched converter. *submited*.

Yuan, G. and S. Banerjee (1998). Border collisions bifurcation in the buck converter. *IEEE Transactions On Circuits and Systems,*.

Zhusubaliyev, Zh.T., E.A. Soukhoterin and E. Mosekilde (2003). Border-collision bifurcations on a two-dimensional torus. *Chaos, Solitons, and Fractals,* pp. 13:1889–1915.